Distributed Optical Fiber Testing for Additive Manufacturing

Brian M. Hlifka, Edward C. Kinzel

Department of Aerospace and Mechanical Engineering, University of Notre Dame,
Notre Dame, IN 46556

Abstract

This paper explores optical fiber's use for in-situ inspection of additive manufacturing. Single-mode SMF-28 optical fiber can be placed on the build plate to monitor the printing process or embedded in the part. Distributed measurements using optical backscattering reflectometry (OBR) resolve the strain along the optical fiber and the temperature. OBR-enabled sensing is demonstrated for the fused filament fabrication (FFF) process. The small diameter (0.125 mm) of SMF-28 lends itself to embedding in FFF prints. This enables laying the fiber into the part, which provides continued sensing for the details in use. Knowledge of the process and the fiber arrangement allows heating from the deposition head to be distinguished from stress-driven strain. Calibration of the fiber arrangement is discussed, as well as a comparison with process modeling.

1. Introduction

Optical fibers have widespread applications in long-distance telecommunications, optical imaging, and advanced optical sensors [1]. This versatility is due to the material's designed optical properties (low losses over long distances), immunity to electromagnetic interference, lightweight construction, compact dimensions, and the ability to accommodate distributed sensor systems [2]. Consequently, distributed fiber sensors are increasingly employed for real-time monitoring of in-process and fabricated materials, providing distinctive capabilities for quality control and performance assessment along the length of the fiber [3]. These distributed sensors can map various physical parameters, including temperature, strain, acoustic vibrations, electric current, and pressure, by detecting changes in light propagation and scattering that result from localized strain profiles along the fiber [4]. This capability to capture strain (both mechanical and by thermal expansion) distributed along the length of the fiber enables in-situ monitoring of a process, but the physical design of the fiber offers additional benefits, particularly in the field of additive manufacturing (AM). Making subtle changes to the design of AM parts allows for optical fiber to be mechanically embedded into the part, which can be used for in-situ recording of the deposition temperature / strain fields. Additionally, the fiber remains mechanically bonded to the part after production allowing for real-time health monitoring of the part in the field, and the extremely small diameters of fibers (0.125 mm) limits the impact on the part's mechanical properties.

The integration of distributed optical fiber sensors into manufactured components, particularly those composed of composite materials, has yielded success. Early endeavors in this domain primarily revolved around Fiber Bragg Gratings (FBGs), which exhibit a longitudinally periodic variation in refractive index within the core of single-mode optical fibers [4]. When employed as embedded sensors within composite materials, FBGs have proven valuable for in-situ measurements across a spectrum of parameters, encompassing strain, temperature, corrosion, vibration, and even the state of cure [5]. However, it is worth noting that the fabrication of FBGs can often be cost-prohibitive due to the intricate microstructure creation within the fiber core, and

their utility is limited to discrete point measurements. Consequently, recent developments have shifted the focus toward deploying distributed optical fiber sensors (DOFS) in fabricated materials, enabling measurements distributed across a manufactured part. DOFS utilizes the innate structural irregularities within optical fibers to capture Rayleigh scattering phenomena along the fibers' length, which can be calibrated to detail temperature and strain measurements. The origin of Rayleigh scattering is related to the refractive index fluctuations caused by density and compositional inhomogeneities in the fiber structure created during the fabrication process when the temperature cools from its glass softening point back down to room temperature [6]. As illustrated in Figure 1, light can travel great distances in two primary directions due to the total internal reflection at the core-cladding interface, which is forward and backward. The Rayleigh backscattered light forms the basis of operation for optical backscattering reflectometry (OBR) measurement techniques.

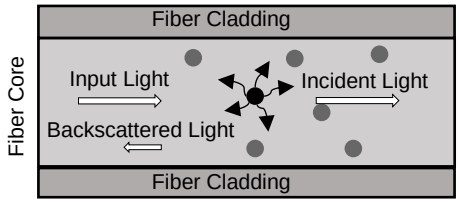

Fig 1. Schematic illustrating Rayleigh scattering phenomenon in optical fibers

Furthermore, the distinctive attributes of DOFS make them highly pertinent to the evolving AM landscape as a quality control measurement technique [7]. The integration of DOFS has garnered substantial attention, particularly in the context of Fused-Filament-Fabrication (FFF) manufactured components. This integration provides AM structures with the capability of real-time monitoring of temperature and strain variations, thus providing crucial insights into the performance and structural integrity of FFF-fabricated objects [8,9]. Recent investigations have delved deeper into optimizing coating adhesion and channel depth techniques for embedding optical fiber sensors within FFF components [10]. These advancements elevate the role of DOFS in AM, pave the way for innovative applications, and enhance quality control standards for applications beyond FFF.

The primary aim of this research article is to formulate a comprehensive set of guidelines geared towards accurately measuring temperature and strain within FFF components. These guidelines are intended to serve as a foundational reference and facilitate integration into complex geometries. The approach will offer insight into the constraints and capabilities associated with integrating DOFS in both AM components and in-process workflow, thereby better understanding their practical utility and limitations. Notably, a Warren truss structure will be employed as an illustrative example. The knowledge derived from these methodologies will be actively used for continuously monitoring strain fluctuations throughout the entirety of the FFF manufacturing process.

2. Measurement Method

The experimental DOFS measurements were performed using Optical Backscattering Reflectometry (OBR). This method commonly employs a tunable laser source (TSL) that emits a continuously changing wavelength within the c-band spectrum over time. The light emitted by this laser source is split into two paths: one measurement and the other for reference. In the measurement path, the light is coupled into the optical fiber sensor, where it interacts with the

optical fiber's natural inhomogeneities, leading to Rayleigh backscattering. This backscattered light serves as the returning signal. Conversely, in the reference path, the light is directed to a beam splitter, where the scattering profiles from both the measurement and reference arms are collected. Subsequently, these two scattering profiles are cross-correlated to assess their similarities, primarily based on the shifts observed. This correlation process translates into measurements of strain and temperature using calibration coefficients that have been empirically determined [11,12,13].

An ODiSI 6100 series interrogator was utilized for all distributed optical fiber measurements based on OBR. This interrogator measures the recorded spectral shift responses, specifically from the intrinsic Rayleigh backscattering signal within an unaltered standard telecommunications-grade optical fiber. These recorded shifts corresponded to variations in both temperature and strain. The concept of spectral shift is described as follows:

$$\frac{\Delta\lambda}{\lambda} = \frac{\Delta f}{f} = K_T \Delta T + K_\varepsilon \Delta\varepsilon \quad (1)$$

In this equation, K_T represents the sum of the thermal expansion and thermo-optic coefficients. Typical values for these coefficients in Germania-doped silica core fibers are $0.55 \times 10^{-6} °C^{-1}$ and $6.1 \times 10^{-6} °C^{-1,}$ respectively. The strain coefficient, $K\varepsilon$, depends on factors such as group index, strain optic sensor components, and Poisson ratio, resulting in a value of 0.787 [14]. Consequently, when measuring temperature, the strain coefficient is disregarded, allowing for the measurement of spectral shifts using the known constant to determine temperature and vice versa with strain.

3. Optical Fiber Sensor Integration in AM

This section provides the guidelines for effectively integrating DOFS into PLA printed specimens through the FFF process. Essential integration techniques for temperature and strain-based measurement applications will be analyzed. All embedded test specimens were produced using the Prusa i3MKS 3D printer, employing a 1.75mm PLA feedstock for each print. Standard printing parameters were maintained, including a nozzle temperature of 215°C and a heated build plate set at 60°C. The layer raster angle was fixed at 45°, and the layer height was set at 0.20mm.

3.1.1. Embedding Optical Fiber in the Warren Truss

In the case of each embedded PLA specimen, printing was paused at a specified height. This pause allowed for the precise placement and integration of the optical fiber into the print. This precision is crucial, as the quality of the integration and resulting signal depends on proper placement security to the part. Therefore, the optical fiber was laid out on the top surface of the sectioned part and was initially secured using Kapton tape. The slack was then removed from this initial layout. External printed jigs were also used to simplify the processes aligning the optical fibers in a known orientation. Once the optical fiber is secured with tape, cyanoacrylate glue is applied to bond the fiber and part together. The epoxy was left to set for ~10 minutes before the printing process continued. The effect of cure duration is not characterized in this study.

To illustrate the capabilities of the integrated optical fiber sensors, a modified Warren truss structure was selected as the representative sample for experimentation. The Warren truss offers more geometric complexity than a tensile test (dog bone) specimen, providing an excellent platform for monitoring temperature and strain variations within a nontrivial design. The standard Warren truss design was slightly modified to allow for the DOFS implementation, incorporating

of a 20mm bending radius to prevent any light leakage from the fiber (refer to Figure 2). When optical fibers are bent excessively, light may escape through the fiber's cladding, which hinders the interrogator's ability to obtain accurate measurements [15].

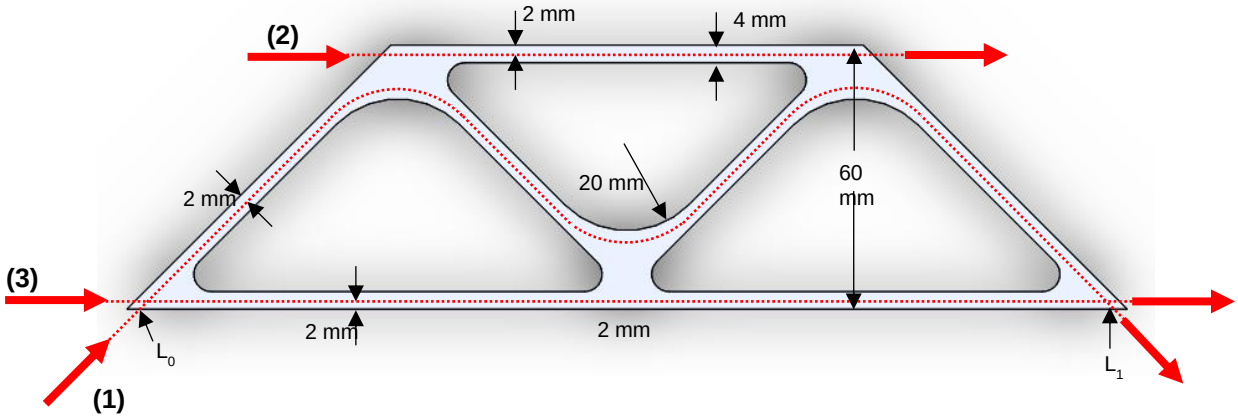

Fig 2. Design of modified Warren truss structure with internal beam bending radius of 20mm

As shown in Figure 2, the SMF-28 fiber was laid out in three geometries over the cross-section of the truss shape. The layout was specifically selected to allow for simultaneous measurements of all members of the shape, while still maintaining full density in the sections of the design with the largest stress concentrations. Each member of the truss was designed to be a 4 × 4 squares with the fiber placed in the center (2 mm above the heat bed, 2 mm from the edge of the part). One of the initial challenges that appeared with using this method was the registration of the fiber embedded in the part compared to the rest of the sensing fiber. To address this registration issue, after the part had been printed, the ODiSI system was used to measure the temperature in the fiber while the tip of a soldering iron (~50°C) was placed at the ends of the embedded fiber (L_0 and L_1 in Figure 1). The ODiSI system detected these temperature changes, with the length of fiber in-between them defining the lengths of embedded fiber.

It is worth noting that since the DOFS technique is designed to measure changes in strain, there can be significant challenges with deconvoluting a combined mechanical – thermal strain profile without a thorough understanding of the interaction between these profiles. This is further complicated by external interactions such as friction between the sample and fiber, as well as the thermal conductivity between the materials. As such, we devised two experimental tests to highlight the design decisions to optimize a produced part for a particular type of strain, aiming to identify the trade-offs between the two methods.

For measuring the mechanical strain internally, it is imperative that the fiber be mechanically well bonded to the surrounding material such that the forces can be effectively transferred to the fiber. As such, this design did not incorporate any designed channels throughout the bulk of the part, instead relying on the adhesive and contact to the part to hold the parts in place. However, to prevent excessive shear stress on the fiber at the edges of the part, a 1×1×1 mm channel was designed at the edge of the part for strain relief. Note that since there are no internal channels designed through the bulk of the part, the fiber must be aligned effectively by hand for embedding into the part, however this can be improved over time with better jigging.

When measuring the temperature profile inside the part, some additional considerations must be made in the design. When the fiber is very strongly bonded to the surrounding material, a change in temperature will not only modify the length of the fiber (thermal strain), but the coefficient of thermal expansion (CTE) mismatch between the fiber (0.5×10^{-6} ε/°C) and PLA (68×10^{-6} ε/°C) is sufficiently large to introduce significant thermal stress in the fiber. This additional tensile stress may compound with the thermal strain, leading to significant errors in the temperature measurements [16,17]. To avoid this phenomenon, the design must be altered such that the fiber is not strongly bonded to the part. This is done by incorporating 1×1 mm channel into the truss (following the desired path displayed in Figure 1). These pre-built channels allow for significantly more accurate placement of the fiber inside the part.

3.1.3. Distributed Strain Measurements

To demonstrate the ability of the DOFS method to capture the internal mechanical strain profile, the samples were tested in a Mark-10 Universal Testing Machine (UTM), in a 3-point bending configuration (Refer to Figure 3).

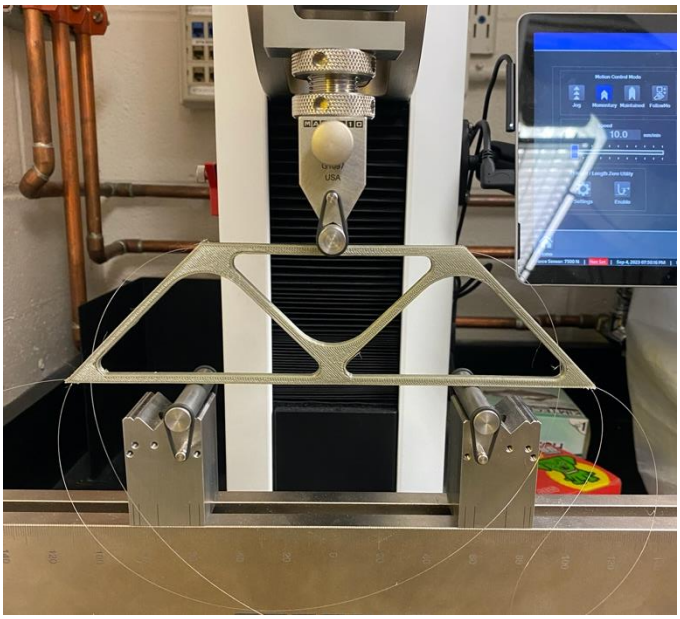

Fig 3. Embedded warren truss structure during three-point bend test with incrementally increasing load

Loads of 10N, 20N, and 30N were applied, showing a linear displacement increase on the top chord of the Warren truss structure based on the in-situ measurements from the optical fiber sensor (see Figure 4). Additionally, the in-situ measurements were compared to simulations conducted using ANSY. It's important to note, that the optical fibers are sensitive to normal strains, therefore, direct comparisons from the top and bottom chord were made based on their given simplified orientations. Also, 3D-viz software was used to visualize the in-situ strain data from the optical fiber sensor distributed along the Warren truss structure. The findings demonstrate a strong correlation between the measured data and the results obtained through ANSYS simulations; however, there are discrepancies for the measured tension in the beam members (see Figure 5).

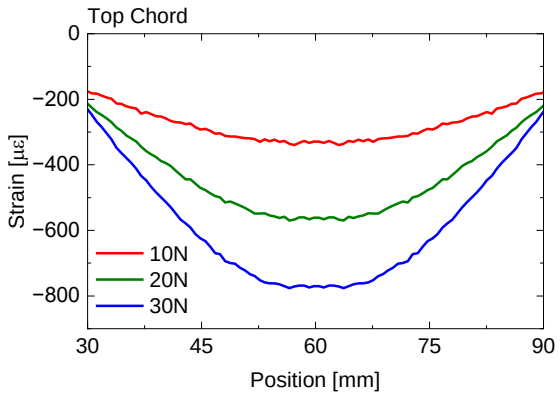

Fig 4. Linear strain response to increasing load on the top chord of the Warren truss

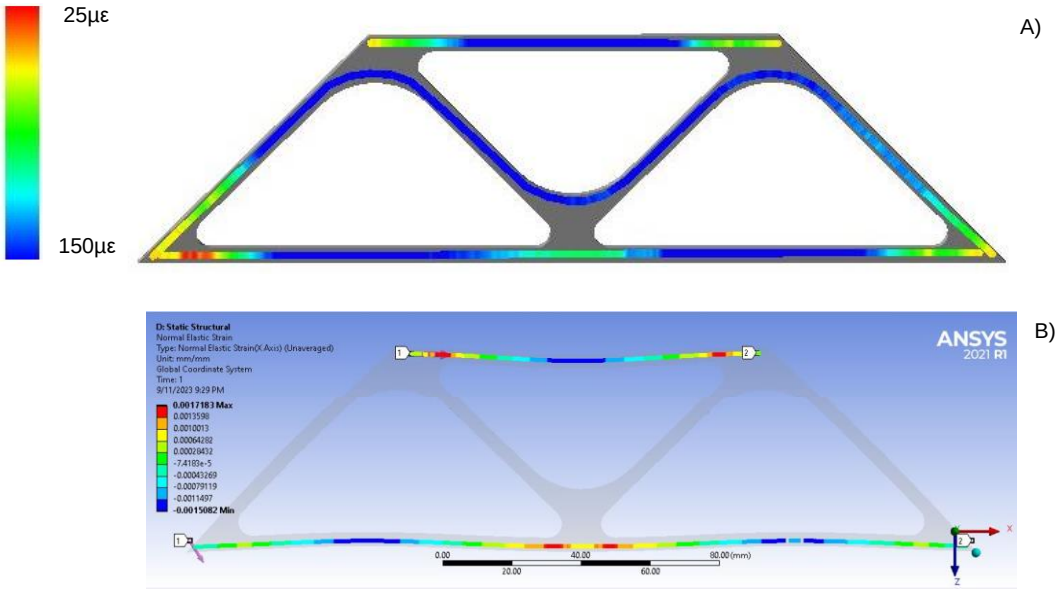

Fig 5. A) In-situ strain response to a 10N applied force in a three-point bend apparatus compared to ANSYS resolved strains for the B) top chord and C) bottom chord of the Warren truss structure

The ANSYS-simulated data, when subjected to a 10N applied load, displays a notable correlation concerning compressive loads. However, there is a substantial inaccuracy in the reflected tension measurements. This discrepancy can primarily be attributed to the placement of the optical fiber within the beam members. Achieving precise optical fiber placement is challenging, particularly when optimizing for strain-related applications, as there are no designated channels for securing the optical fiber sensors within the beam members.

Precision in placement plays a pivotal role in obtaining measurements that closely match simulation results. In this context, each optical fiber was intended to be positioned at the neutral axis of each member, where the beam's width measures 4mm. However, achieving this ideal placement posed challenges and uncertainties, particularly at the edges of the structure. The primary concern with optical fibers structure's edges is the potential for displacement or increased stress due to overlap, which can result in issues such as light leakage or fractures. There were instances in the Warren truss structure where optical fibers overlapped with the internal structural

beam members and the bottom chord, presenting challenges as the optical fibers became susceptible to breakage or displacement during the printing process.

To address this issues, 1mm x 1mm x 1mm channels were introduced at the edges of each structural member. These channels serve a dual purpose: they permit optical fibers overlap and ensure precise placement within the structure without compromising their sensitivity to strain. It's worth noting that the use of these channels at the edges introduce minor variations in strain measurements between the edges of each optical fiber, potentially affecting the resulting strain measurements within the truss structure. Moreover, concerns may also arise regarding the effectiveness of the cyanoacrylate glue in bonding the optical fiber to the PLA specimen. A need exists for more comprehensive and in-depth investigations to gain thorough understanding of how these channels, and choice of adhesive can influence the resulting strain measurements.

3.1.3. Distributed Temperature Measurements

In addition to investigating strain measurements, this study also delved into optimizing the warren truss structure for temperature monitoring. For this purpose, a thermal camera was employed to capture temperature variations across the Warren truss structure. This enabled comparison from the thermal data obtained through the camera with the distributed measurements obtained from the optical fiber sensor.

To optimize the Warren truss structure for temperature measurements, one critical aspect was considered, which was ensuring the optical fiber's precise placement within the structure. This optimization process included channel depths of 1mm x 1mm along each structural member. These channels played a crucial role in providing the optical fiber with sufficient space, mitigating the potential challenges arising from the differences in coefficients of thermal expansion (CTE) between the silica cladding of the optical fiber and the PLA material used in the truss structure.

To facilitate temperature measurements within the Warren truss structure, an Optris PI 640i infrared camera was employed. This camera allowed precise temperature data to be captured across the truss structure, providing a valuable benchmark for comparing the distributed temperature measurements obtained from the embedded optical fiber sensors. Also, adjustments to the emissivity were changed to 0.92 to match the molten polymer [18].

Controlled temperature experimentation was conducted to facilitate a comparison between the thermal camera and the DOFS. The embedded Warren truss structure was exposed to an external temperature source generated by a Corning PC-400D digital hot plate. A predetermined temperature of 50°C was established as the reference point for this comparative analysis. The placement of the Warren truss structure on the hot plate was strategically chosen to accentuate the temperature variations within the structure. By positioning and securing the truss structure at the center of the hot plate, it was ensured that the central region would experience the highest temperature, with temperatures diminishing towards the outer portions of the structure. This arrangement aimed to provide a clear demonstration of how temperature gradient would manifest across the truss.

Like the approach taken for strain measurements, temperature changes were monitored using a known temperature source, such as the thermal camera, while the distributed optical fiber measurements were visualized and analyzed using 3D-viz software. The results, presented in Figure 6, reveal a significant level of correlation between the temperature data obtained from the thermal camera and the optical fiber sensor.

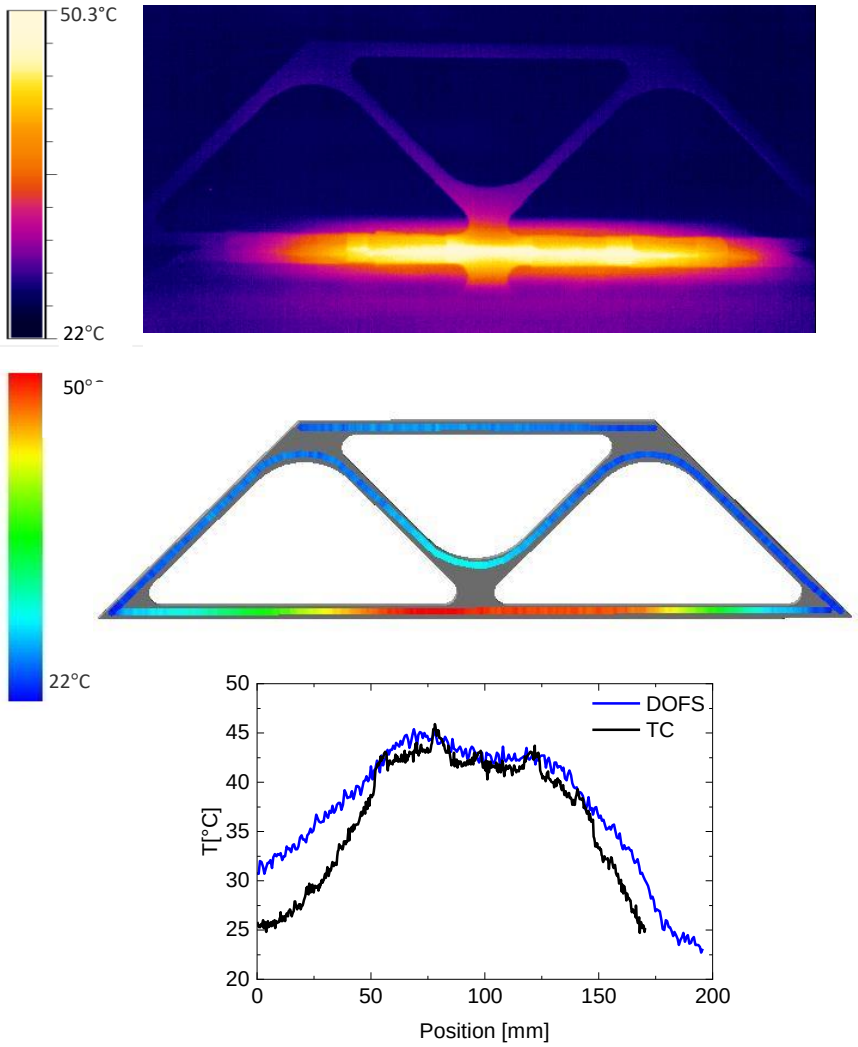

Fig 6. Temperature response comparison between the thermal camera and embedded optical fiber sensors when exposed to 50°C

The results obtained from the temperature optimization highlight the enhanced capabilities of the integrated optical fiber sensor for temperature measurements within complex structures like the Warren truss. Incorporating embedment channels significantly improves measurement accuracy compared to a Warren truss structure optimized for strain sensing. It is essential to note that the differences in the CTE between the optical fiber and PLA introduce additional strain changes within the part as the temperature fluctuates. The fundamental principles underlying the ODiSI 6100 series interrogator remain consistent, as all temperatures and strain measurements rely on spectral shifts in Rayleigh scattering sites transitioning from their initial state to a stressed state

induced by temperature or strain variations. These variations in measurement accuracy are exemplified in the results obtained from the two fabricated truss samples exposed to a temperature of 50°C (Refer to Figure 7).

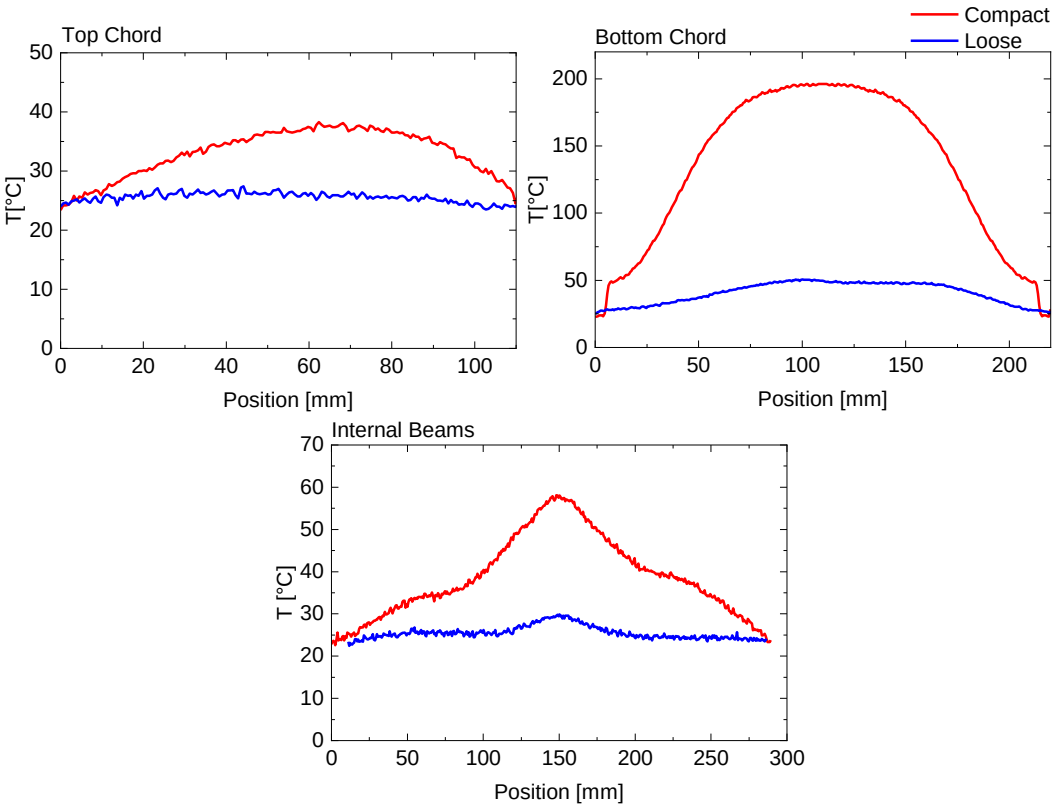

Fig 7. Temperature measurements in embedded Warren truss samples illustrate two interface conditions: compact and loose when subjected to a temperature of 50°C. The loose interface sample features structural channels

The Warren truss sample that was fabricated without the use of channel exhibits superior bonding to the specimen when compared to the fiber placed with the designated channel. Consequently, the difference in CTE for the PLA affects the resulting temperature measurement in the strain optimized sample. As the temperature rises, the PLA material expands, leading to a shift in Rayleigh backscattering that simultaneously measures both temperature and strain. Therefore, there are ongoing challenges in applying optical fiber to accurately capture both temperature and train measurements. This is because the ODiSI system measures a pure shift of Rayleigh scatter and correlates it to ither a strain or temperature, the system cannot simultaneously measure both. As a result, there are inherent discrepancies in measurements based on the specified application.

4. Integration with the FFF Process

The refined approach for strain measurement has been successfully applied to more intricate structures, such as the warren truss. The insights gained from this experience can be directly implemented within an additive manufacturing (AM) process. To illustrate this capability, the placement of an optical fiber on the build plate has been demonstrated, showing its potential to monitor strain and temperature fluctuations. Masking tape secured the optical fiber, ensuring its stability and proper positioning throughout the FFF printing process (refer to Figure 8).

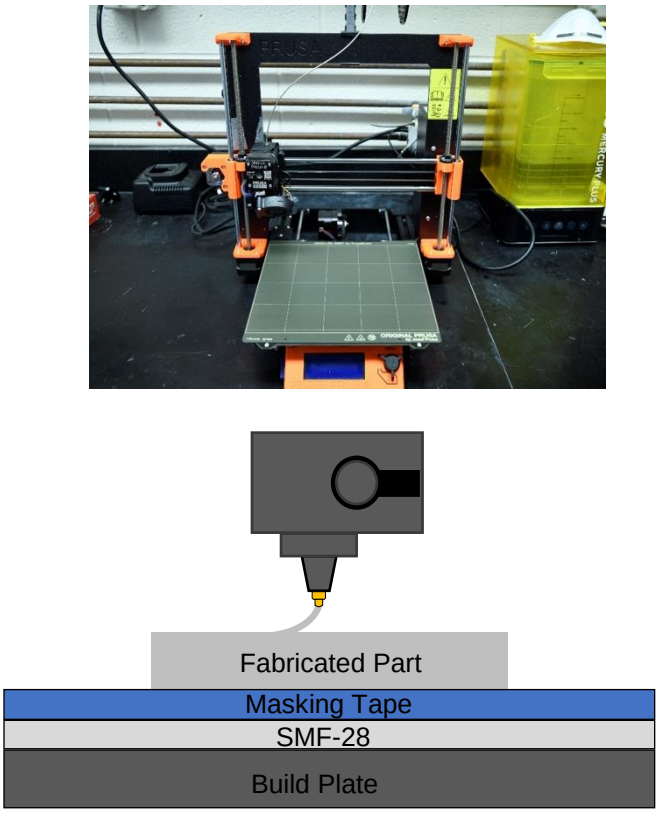

Fig 8. Prusa i3MKS printer and schematic depicting the configuration of the optical fiber on the build plate

When subjected to an applied thermal load resulting from the heating and cooling of molten PLA material, the optical fiber is sensitive to thermal and strain changes from the part. A 200mm x 12.7mm test specimen was printed with the optical fiber aligned along its neutral axis to establish a baseline measurement for incorporating the optical fiber onto the build plate. The spectral shift was measured for each layer, observing a decreasing negative shift peak after each subsequent layer (refer to Figure 9). The test print adhered to standard printing conditions, including a raster angle of 45° and a layer height of 0.20mm.

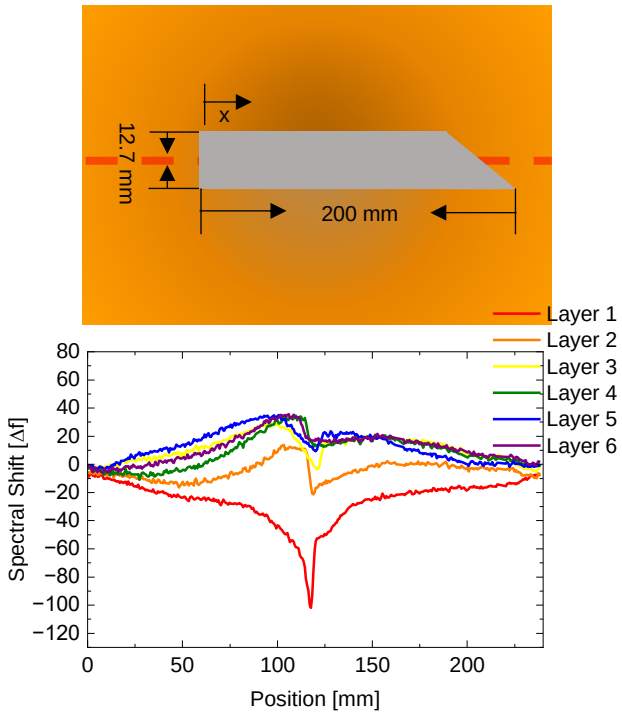

Fig 9. Spectral shift response for layer-by-layer deposition for a 200mmx12.7mm test specimen

The optical fiber response stabilizes after approximately five layers, equivalent to a height of 1mm. However, there is a limitation to integrating the optical fiber on the build plate, as its sensitivity diminishes progressively with the increasing distance from the build plate due to the reduced thermal load. Nevertheless, the optical fiber continues to effectively detect external shear forces resulting from the interaction between the nozzle and the printed part. The optical fiber's sensitivity to normal forces along its designated position on the bed allows it to perceive shear forces induced by the nozzle interaction with the part. This aspect is intriguing because regardless of the printed part's height, the induced shear force remains constant, as it is a relationship between the force and area of the print.

$$\tau = \frac{F}{A} \tag{2}$$

To verify the consistency of shear forces, a test specimen measuring 12.7mm x 12.7mm x 38.1mm was printed, where the optical fiber was secured to the build plate along the neutral axis of the part. This test aimed to demonstrate that a constant shear force of 5N remained uniform, irrespective of the height at which it was applied (refer to Figure 10). The forces were applied using a fish scale, and a soldering iron was employed to create an area for the fish scale to exert force, resulting in an approximate 5N force.

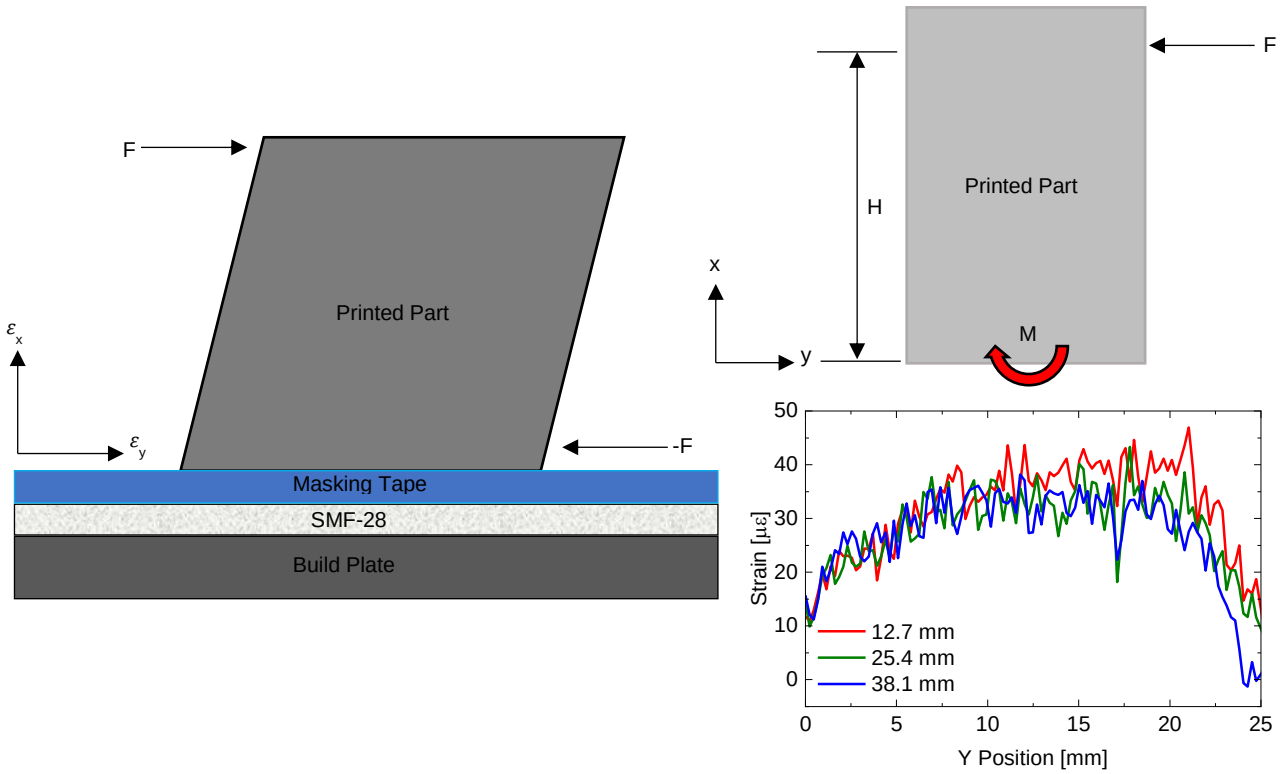

Fig 10. Illustration of shear forces applied to a printed component and corresponding strain measurements for an applied force of approximately 5N

The resultant shear forces from an applied load are the same despite the height where the force is applied. However, the amount of force required to remove the printed part decreases as the height increases for the part. It's important to note that before the removal of the part with the inclusion of masking tape, the printed piece is attached to the tape, so with an increasing shear force, there will be an equal and opposing force in parallel to the direction of the load and an opposite normal force, where a spike in strain will be shown before completely being ripped off the build plate. This phenomenon was exemplified using the same printed specimen. However, a load of 12.8N was applied at a height of 12.7mm, and a load of 14.2N was applied at 25.4mm. The results reveal a strain profile with significant peaks corresponding to the opposing forces acting on the printed part (see Figure 11).

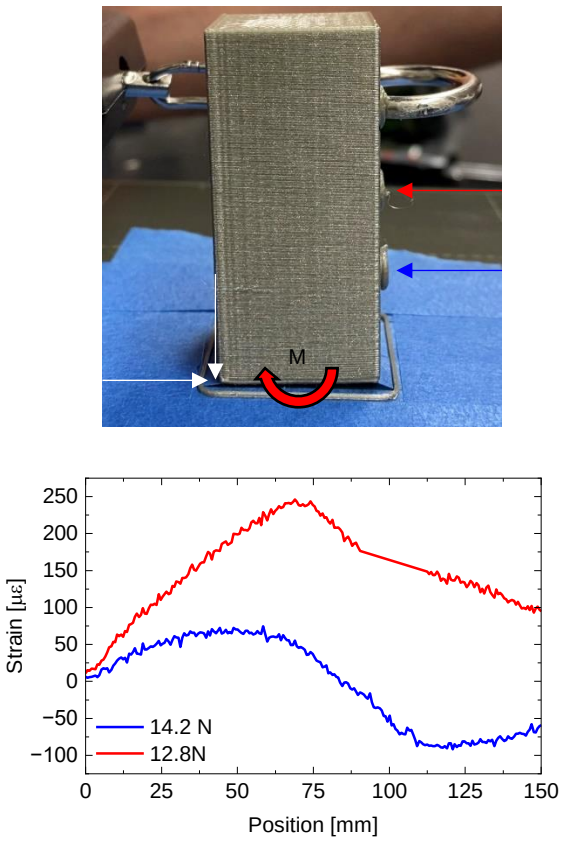

Fig 11. Strain response of optical fiber to external loads at different heights with varying forces

Even with a lower load at greater heights, a substantial opposing force is generated to retain the part of the build plate. This extends the utility of integrated optical fiber beyond the initial few printed layers. Nonetheless, further comprehensive investigations are required to enhance its robustness. These studies could establish a correlation between the measured strain response and the point at which potential detachment from the bed or failure might occur.

5. Conclusions

Optical fiber sensors have demonstrated their versatility as invaluable tools for real-time monitoring in additive manufacturing (AM) processes, providing critical data on temperature and strain. Their unique capacity to capture distributed physical information along the length of the fiber offers valuable insights into material behavior while maintaining the structural integrity of the components. Specifically, distributed optical fiber sensors (DOFS) have emerged as promising alternatives to traditional discrete point sensors like Fiber Bragg Gratings (FBGs). DOFS enables measurements to be distributed across the entirety of the manufactured part, thereby enhancing the capabilities for quality control and performance assessment in AM components.

Therefore, ensuring the precise placement and secure attachment of optical fibers within AM components is imperative to guarantee accurate measurements. The optimization of temperature measurements within the Warren truss structure exemplifies the enhanced potential of integrated optical fiber sensors. Incorporating embedment channels has notably elevated measurement accuracy compared to structures primarily tailored for strain sensing.

Moreover, further research endeavors are warranted to strengthen the robustness of optical fiber integration within AM processes. These comprehensive studies should strive to establish correlations between recorded strain responses and the critical point at which potential detachment from the build plate or failure may occur. This will provide a comprehensive understanding of these sensors' practical utility and limitations in additive manufacturing.

6. References

[1] P. Lu, et al, "Distributed optical fiber sensing: review and perspective," Applied Physics Reviews **6** (2019).

[2] B. Lee, "Review of the present status of optical fiber sensors," Optical Fiber Technology **9**(2), 57-79 (2003). [3] A. Rogers, "Distributed optical-fiber sensing," Measurement Science and Technology **10**(8), (1999).

[3] A. Rogers, "Distributed optical-fibre sensing," Measurement Science and Technology **10**(8), (1999).

[4] V.M. Murukeshan, P.Y. Chan, L.S. Ong, L.K. Seah, "Cure monitoring of smart composites using Fiber Bragg Gratings based embedded sensors," Sensors and Actuators A: Physical **79**(2), 153-161 (2000).

[5] K.S.C Kuang, R. Kenny, M.P. Whelan, W.J. Cantwell, P.R. Chalker, "Embedded fibre Bragg grating sensors in advanced composite materials," Composites Science and Technology **61**(10), 1379-1387 (2001).

[6] G. P. Agrawal, Nonlinear Fiber Optics (Academic Press, 2013).

[7] Y. Fu, A. Downey, L. Yuan, A. Pratt, Y. Balogun, "In-situ monitoring for fused filament fabrication process: A review," Additive Manufacturing **38**, 101749 (2021).

[8] S. Wang, K. Lasn, C.W. Elverum, D. Wan, A. Echtermeyer, "Novel in-situ strain measurements in additive manufacturing specimens by using Optical Backscatter Reflectometry," Additive Manufacturing **32**, 101040 (2020).

[9] S. Wang, K. Lasn, "Integration of optical fiber sensors by material extrusion 3-D printing – the effect of bottom interlayer thickness," Materials & Design **221**, 110914 (20

[10] F. Mashayekhi, J. Bardon, Y. Koutsawa, S. Westermann, F. Addiego, "Methods for embedding fiber Bragg grating sensors during material extrusion: Relationship between the interfacial bonding and strain transfer," Addit. Manuf. **68**, (2023).

[11] Z. Ding, et al. "Distributed optical fiber sensors based on optical frequency domain reflectometry: a review," Sensors **18**(4), 1072 (2018).

[12] Kreger, et al. “Optical frequency domain reflectometry: principles and applications in fiber optic sensing,” Proc. SPIE 9852-98520T (2016).

[13] Kreger, S. “Distributed strain and temperature sensing in plastic optical fiber using Rayleigh scatter,” Proc. SPIE 7316, Fiber Optic Sensors and Applications VI, 73160A (2009).

[14] S.T. Kreger, D.K. Gifford, M.E. Froggatt, A.K. Sang, R. G. Duncan, M.S. Wolfe, B.J. Soller, “High-resolution distance distributed fiber-optic sensing using Rayleigh backscatter,” SPIE 65301R (2007).

[15] K. Hurokawa, “Optical Fiber for high-power optical communication,” Crystals **2**(4), 1382-1392 (2012).

[16] B. Deng, Y. Shi, F. Yuan, “Investigation on the structural origin of low thermal expansion coefficient of fused silica,” Materialia **12**, 100752 (2020).

[17] A. Botean, “Thermal expansion coefficient determination of polylactic acid using digital image correlation,” EENVIRO **32,** 01007 (2018).

[18] R. Badarinath, V. Prabhu, “Real-time sensing output polymer flow temperature and volumetric flowrate in fused filament fabrication process,” Materials (Basel) **15**(2), 618 (2022).